articles

molecular pharmaceutics

Simultaneous Release and ADME Processes of Poorly Water-Soluble Drugs: Mathematical Modeling

Gabriele Grassi,[†,‡] Dritan Hasa,[§] Dario Voinovich,[§] Beatrice Perissutti,[§] Barbara Dapas,[†] Rossella Farra,[‡] Erica Franceschinis,[||] and Mario Grassi*[,⊥]

Department of Life Sciences, University of Trieste, Via Giorgieri, 1, I-34127, Department of Medical, Technological and Translational Sciences, University Hospital of Cattinara, Trieste, Italy, Department of Pharmaceutical Sciences, University of Trieste, Piazzale Europa 1, I-34127 Trieste, Italy, Department of Pharmaceutical Sciences, University of Padova, Via F. Marzolo 5, I-35131 Padova, Italy, and Department of Materials and Natural Resources, University of Trieste, Via Alfonso Valerio, 2, I 34127 Trieste, Italy

Received April 23, 2010; Revised Manuscript Received July 9, 2010; Accepted July 20, 2010

Abstract: The importance of studying oral drug absorption is well recognized by both research facilities/institutions and the pharmaceutical industry. The use of mathematical models can represent a very profitable and indispensable tool to understand oral drug absorption. Indeed, mathematical models can verify the correctness of the mechanisms proposed to describe drug release, absorption, distribution and elimination thus reducing the number of expensive and time-consuming experiments. In this paper we develop a mathematical approach able to model both the polymeric particle mediated delivery and the gastrointestinal absorption−metabolism−excretion (ADME) of a given drug. As a model drug a poorly water-soluble drug (vinpocetine) in both the amorphous and nanocrystalline state is considered. The delivery system is obtained by drug cogrinding with a polymer (cross-linked polyvinilpyrrolidone). As the proposed mathematical model can properly fit the *in vivo* data on the basis of information obtained *in vitro*, it represents a powerful theoretical tool connecting *in vitro* and *in vivo* behavior.

Keywords: Mathematical modeling; poorly soluble drugs; oral administration

1. Introduction

Many pharmaceutical systems are essentially made up of a polymeric carrier hosting the active agent (drug) inside its three-dimensional network.[1,2] Especially in the case of oral administration, they are often prepared as particulate systems since these forms present remarkable advantages over the single unit devices. The easier dispersion inside the stomach reflects into an appreciable reduction of the local drug concentration which is usually responsible for gastric irritation.[3] Moreover, they are very versatile and powerful as drug loading into cross-linked polymers can represent a profitable tool to increase the drug dissolution rate in aqueous media and, thus, the bioavailability of slightly water-soluble crystalline drugs.[4] Indeed, for example, by means of solvent swelling, cogrinding techniques or supercritical CO_2,[5−7] the drug can be loaded inside the polymeric network in the form

* Corresponding author. Mailing address: Department of Materials and Natural Resources (DMNR), University of Trieste, Via Alfonso Valerio, 2, I 34127 Trieste, Italy. E-mail: mariog@dicamp.univ.trieste.it. Tel: 0039 040 5583435. Fax: 0039 040 569823.

[†] Department of Life Sciences, University of Trieste.

[‡] University Hospital of Cattinara.

[§] Department of Pharmaceutical Sciences, University of Trieste.

[||] University of Padova.

[⊥] Department of Materials and Natural Resources, University of Trieste.

(1) Lee, P. I. Diffusion-Controlled Matrix Systems. In *Treatise on Controlled Drug Delivery*; Kydonieus, A., Ed.; Marcel Dekker Inc.: New York, Basel, Hong Kong, 1992; Chapter 3.

(2) Peppas, N. A. Mathematical Models for Controlled Release Kinetics. In *Medical Applications of Controlled Release: Applications and Evaluations*; Langer, R. S., Wise, D. L., Eds.; CRC Press: Boca Raton, 1984; vol. II, pp 169−187.

(3) Tapia, C.; Buckton, G.; Newton, J. M. Factors influencing the mechanism of release from sustained release matrix pellets, produced by extrusion/spheronisation. *Int. J. Pharm.* **1993**, *92*, 211–218.

10.1021/mp1001334
Published on Web 07/20/2010

of macrocrystals, nanocrystals and amorphous state. Interestingly, drug nanocrystals and the amorphous state are characterized by increased water solubility (in virtue of their small crystal size, strictly connected to small curvature radii) with respect to macrocrystals and this, obviously, reflects into increased bioavailability.[6] Unfortunately, however, thermodynamically speaking, drug nanocrystals and the amorphous state are, usually, far from being stable compared to the lifetime required for a pharmaceutical product (months or years). Accordingly, the addition of at least one more component (stabilizer), usually a polymer, is required. Indeed, drugs can interact, for example, via van der Waals forces or hydrogen bonds, with the stabilizer yielding to pharmaceutically stable products thus conserving their activation for a long time.[6] In addition, in the case of polymeric stabilizers, the physical presence of the polymeric chains hinders macrocrystal formation since macrocrystals can form and grow as long as the network meshes are sufficiently wide. Obviously, upon contact with the aqueous external release environment (gastrointestinal (GI) fluids), the stabilizer action ends and drug nanocrystals or the amorphous state tends to come back to the more stable form (recrystallization), i.e. to the macrocrystal condition, according to different kinetics depending on the carrier and drug type. Accordingly, the release process takes place as the drugs were characterized by a decreasing solubility.[4] Interestingly, despite the recrystallization phenomenon, the average solubility and, thus, bioavailability of the drug are neatly increased.[7]

Whereas the mathematical modeling of drug release from an ensemble of polydisperse polymeric particles has been matched in literature,[4] few modeling attempts have been performed on the combination of drug release, absorption, elimination and metabolism (ADME).[8,9] The reasons for this probably rely on the mathematical difficulties connected to this task. However, as recently pointed out by Siepmann,[10] one of the major challenges to be addressed in the future is the combination of mechanistic theories describing drug release out of the delivery systems with mathematical models quantifying the subsequent drug transport within the human body in a realistic way. Accordingly, the aim of this paper is to present a mathematical model able to account for (1) the *in vivo* drug release from an ensemble of polymeric particles containing a drug in the amorphous and/or nanocrystalline condition, (2) the simultaneous drug absorption from the GI mucosa and (3) the final accumulation/elimination/metabolism in the blood. The proposed mathematical model is applied to study the *in vitro* and *in vivo* release of a poorly water-soluble drug (vinpocetine) from a system realized by cogrinding for three hours micronized cross-linked polyvinylpyrrolidone (PVP-clm) and vinpocetine (w/w ratio 4:1). Indeed, preliminary *in vivo* tests on rats proved the efficacy of this system in improving the bioavailability of vinpocetine.[11]

2. Experimental Section

2.1. Materials. Vinpocetine, a kind gift from Linnea SA (Riazzino-Locarno, CH), is a semisynthetic derivative of the *Vinca minor* L. alkaloid vincamine.[12] VIN is base-type drug ($pK_b = 7.1$) whose solubility in buffer (0.2 M KH_2PO_4/0.2 M NaOH (pH 7.4) at 37 °C) is 1.6 $\mu g/cm^3$.[13] It has been shown to improve cerebral circulation and metabolism in the treatment of various types of cerebrovascular circulatory disorder, e.g. cerebral infarction, cerebral hemorrhage residual etc. It is mainly used as oral dosage forms, usually in tablets, containing 5 mg of active ingredient, with a daily dosage regimen that can vary between 5 mg and 20 mg for three consecutive days.[14] However, existing formulations exhibit poor bioavailability (~6.7%)[15,16] and poor absorption[17] due to its scarce aqueous solubility, wettability and extensive metabolism during first pass. Micronized crospovidone (PVP-clm) was purchased by BASF/Euphar (Milano, Italy). All other chemicals, of analytical grade, and solvents of HPLC grade, were provided by Carlo Erba (Milan, Italy). The delivery system was prepared by cogrinding for three hours the drug and the polymer (1:4 w/w ratio) in a planetary mill Fritsch P5 (Pulverisette, Contardi Fritsch s.r.l., Milan, Italy).[11]

(4) Grassi, M.; Grassi, G.; Lapasin, R.; Colombo, I. *Understanding drug release and adsorption mechansims: a phyisical and mathematical approach*; CRC Press: Boca Raton, 2007.
(5) Grassi, M.; Colombo, I.; Lapasin, R. Drug release from an ensemble of swellable crosslinked polymer particles. *J. Controlled Release* **2000**, *68*, 97–113.
(6) Colombo, I.; Grassi, G.; Grassi, M. Drug Mechanochemical Activation. *J. Pharm. Sci.* **2009**, *98*, 3961–3986.
(7) Debenedetti, P. G.; Tom, J. W.; Yeo, S. D. Application of supercritical fluids for the production of sustained delivery devices. *J. Controlled Release* **1993**, *24*, 27–44.
(8) Di Muria, M.; Lamberti, G.; Titomanlio, G. Modeling the pharmacokinetics of extended release pharmaceutical systems. *Heat Mass Transfer* **2009**, *45*, 579–589.
(9) Di Muria, M.; Lamberti, G.; Titomanlio, G. Physiologically Based Pharmacokinetics: A Simple, All Purpose Model. *Ind. Eng. Chem. Res.* **2010**, *49*, 2969–2978.
(10) Siepmann, J.; Siepmann, F. Mathematical modeling of drug delivery. *Int. J. Pharm.* **2009**, *364*, 207–212.
(11) Hasa, D. Attivazione meccanochimica di un composto contenente vinpocetina; Graduate thesis, University of Trieste, Department of Pharmaceutical Sciences, 2009.
(12) Lorincz, C.; Szasz, K.; Kisfaludy, L. The synthesis of ethyl apovincaminate. *Arzneim. Forsch./Drug Res.* **1976**, *26*, 1907–1908.
(13) Ribeiro, L. S. S.; Falcao, A. C.; Patricio, J. A. B.; Ferreira, D. C.; Veiga, F. J. B. Cyclodextrin multicomponent complexation and controlled release delivery strategies to optimize the oral bioavailability of vinpocetine. *J. Pharm. Sci.* **2007**, *96*, 2018–2028.
(14) Szatmari, S. Z.; Whitehouse, P. J. Vinpocetine for cognitive impairment and dementia. *Cochrane Database Syst. Rev.* **2003**, *1*, CD003119.
(15) Grandt, R.; Beitinger, R.; Schateltenbrand, R.; Braun, W. Vinpocetine pharmacokinetics in elderly subjects. *Arzneim. Forsch./Drug Res.* **1989**, *39*, 1599–1602.
(16) Szakacs, T.; Veres, Z.; Vereczkey, L. In vitro-in vivo correlation of the pharmacokinetics of vinpocetine. *Pol. J. Pharmacol.* **2001**, *53*, 623–628.
(17) Kata, M.; Lukacs, M. Enhancement of solubility of vinpocetine base with γ-cyclodextrin. *Pharmazie* **1986**, *41*, 151–152.

2.2. *In Vitro* Test. Release tests, performed in triplicate, were carried out in 250 cm^3 of 0.2 M KH_2PO_4/0.2 M NaOH (pH 7.4) at 37 °C. Two different release tests were performed. In the first case, at time zero, 25 mg of the coground system (corresponding to 5 mg of vinpocetine) was added to the release environment while, in the second case, 12.5 mg of the coground system (corresponding 2.5 mg of vinpocetine) was added to the release environment. Uniformity conditions were ensured by means of an impeller (rotational speed 200 rpm). The use of a fiber optic apparatus (HELLMA, Italy), connected to a diode array spectrophotometer (ZEISS, Germany, wavelength 270.19 nm), allowed the determination of vinpocetine concentration without perturbing the release environment (each release test lasted 180 min). Moreover, this methodology allowed the problem connected to drug concentration measurement in the presence of a dispersion of solid particles to be easily overcome. Indeed, the UV spectrophotometer, recording the UV absorption spectrum in the wavelength range 210−620 nm, can automatically subtract the scattering absorption due to the polymeric particles from the vinpocetine maximum UV absorption occurring at 270.19 nm. As the scattering effect does not depend on the wavelength in the wavelength range considered, it was evaluated at 500.49 nm, i.e. very far from 270.19 nm.

2.3. *In Vivo* Test. A 10 mg vinpocetine dose (corresponding to 50 mg of coground system) was orally administered to eight healthy male volunteers, aged between 25 and 50 years and weighing on average 77 kg. The test was subdivided in two steps. In the first step, the coground system was administered to five volunteers while the second step regarded the last three volunteers and was performed 4 months later. Written informed consent was signed by each subject participating in the study. The research followed the tenets of the Declaration of Helsinki promulgated in 1964 and was approved by the institutional human experimentation committee. All the volunteers had normal hepatic and renal function. All subjects were asked not to take any drugs before and to fast from 12 h before administration until lunch on the treatment day. They were also not allowed to smoke and not to take coffee or alcoholic beverages 12 h before drug administration. The subjects were all given a standard lunch 5.5 h after the dosing and were allowed to drink water during the treatment period. Blood samples (5 mL) were drawn at 0.5, 1, 2, 4, and 6 h after administration for the first five volunteers while blood samples (5 mL) were drawn at 0.25, 0.5, 1, 1.5, 2, 3, 4, and 6 h after administration for the remaining three volunteers. Each sample was collected in a heparinized tube; the plasma was then immediately separated by centrifugation (at 4000 rpm for 45 min) and stored at −20 °C until analysis. The determination of vinpocetine concentration in the plasma implied the addition of 600 μL of methanol to 200 μL of plasma. This mixture was vortexed for 10 min. After centrifugation (5000 rpm for 6 min), 5 μL of the organic solution was assayed by a validated HPLC analysis with mass spectrometry detection.[18] The HPLC system consisted of a Varian LC212 with a 500-MS IT mass detector. The chromatographic separation was conducted at room temperature, using a Varian C 18 Polaris column (3 μm, 2.0 × 50 mm). The mobile phase was composed of water with 0.1% formic acid (solvent A) and acetonitrile (solvent B). Isocratic conditions were used with 57:43 A:B; total run time was 3 min. The flow rate was 200 μL/min. MS conditions: ESI (positive mode), needle voltage 5350 V, drying gas temperature was 400 °C, capillary voltage was set to 100 V and RF loading was set to 100%, nebulizer gas pressure was 25 psi; drying gas pressure was 15 psi. The detector was set to monitor $m/z = 290-390$. The calibration curve for vinpocetine ranged from 14 to 200 ng/mL (plasma). The limit of quantification was 2 ng/mL. The precision and accuracy were under 3% for all calibration points.

3. Mathematical Modeling

3.1. *In Vivo* Drug Release, Absorption, Distribution, Metabolism and Elimination. The complete description of all the phenomena involved in the release kinetics from drug loaded particulate systems is not a trivial task as release kinetics is ruled by many phenomena such as matrix swelling and erosion, drug dissolution, recrystallization and diffusion, drug−matrix network interactions, drug distribution and concentration inside the matrix and, finally, particle size distribution. The scenario is made more complex when the modeling aim is not limited to the description of the release kinetics in the release environment (GI fluids), but it also has to describe drug absorption (by the GI tract mucosa), distribution (among blood, tissues and organs), metabolization and elimination, i.e, the so-called ADME processes. Indeed, the mathematical model must account for drug permeation through cellular membranes and distribution/elimination in the blood, tissues and organs.

In light of the complexity of the process, model building could be based on the following simplifying assumptions:[4,5,19] (1) the GI tract is considered as a well stirred environment (uniform drug concentration in its liquid volume), (2) drug release in GI fluids is substantially equal to *in vitro* drug release (to make this assumption as reasonable as possible, the definition of more and more sophisticated *in vitro* techniques to test the drug release is required), (3) drug solubility (C_s) in the release environment (GI fluid) and drug permeability (P) are constant along the GI tract, (4) even if more complex approaches could be considered, for the sake of simplicity, drug pharmacokinetics is represented by two

(18) Vlase, L.; Bodiu, B.; Leucuta, S. E. Pharmacokinetics and comparative bioavailability of two vinpocetine tablet formulations in healthy volunteers by using the metabolite apovincaminic acid as Pharmacokinetic parameter. *Arzeim. Forsch./Drug Res.* **2005**, *55*, 664–668.

(19) Quintavalle, U.; Voinovich, D.; Perissutti, B.; Serdoz, F.; Grassi, G.; Dal Col, A.; Grassi, M. Preparation of sustained release co-extrudates by hot-melt extrusion and mathematical modelling of in vitro/in vivo drug release profiles. *Eur. J. Pharm. Sci.* **2008**, *33*, 282–293.

"external" compartments, blood and tissues, and the central one, i.e. the GI environment, and (5) the polymeric powder is made up of spherical particles that do not undergo significant erosion. In addition, the particle size distribution in the dry state (this corresponding to the initial powder condition) is supposed to be conveniently described by the Weibull equation,[20] even if, in principle, any distribution equation could be used:

$$\frac{V}{V_0} = 1 - e^{-[2(R_p - R_{min})/\eta]^\delta} \quad (1)$$

where R_p and R_{min} are the generic particle radius and the minimum particle radius, respectively, η and δ are two parameters regulating the Weibull size distribution, and V_0 and V are the total volume occupied by the ensemble of polymeric particles and the volume occupied by particles having a radius lower than or equal to R_p, respectively.

In order to describe the whole release process, two mass balances, referred to the solvent (water or GI fluid) uptake and to the drug release, respectively, must be taken into consideration and solved for all the particles. Although the model accounts for particle volume increase due to polymer swelling, it is assumed that the drug diffusion process does not reflect in any volume variation. Accordingly, the solution of the problem may be achieved by first solving the solvent mass balance and then, once the solvent concentration profile is known inside each particle, by solving the drug mass balance. Due to the viscoelastic nature of the polymer/solvent system, solvent uptake needs to be described according to a non-Fickian approach. Among the huge variety of models proposed in the past,[4] that proposed by Camera-Roda and Sarti provides a simple but reasonable way to account for the relaxation of viscoelastic materials in the analysis of diffusional problems.[21] This theory assumes that the global solvent flux J can be subdivided into two contributions:

$$J = J_f + J_r \quad (2)$$

where J_f represents the fickian contribution to the solvent flux, while the second term J_r is the relaxation contribute representing the viscoelastic nature of the polymer−solvent system. In a spherical coordinate system, J_f and J_r read

$$J_f = -D_0 \frac{\partial C_p}{\partial R} \quad (3)$$

$$J_r = -D_r \frac{\partial C_p}{\partial R} - \tau \frac{\partial J_r}{\partial t} \quad (4)$$

where C_p represents solvent concentration at the radial position R, t is the time, D_0 is the solvent diffusion coefficient in the dry polymeric network, D_r is the diffusion coefficient of the non-Fickian flux and τ is the relaxation time characteristic of the polymer−solvent system. D_r and τ dependence on local solvent concentration is given by

$$D_r = D_{eq}\, e^{g(C_{pj} - C_{peq})} - D_0 \quad (5)$$

$$\tau = \tau_{eq}\, e^{f(C_{peq} - C_{pj})} \quad (6)$$

where C_{peq} is the solvent concentration in the completely swollen polymeric network (thermodynamic equilibrium), τ_{eq} and D_{eq} are the relaxation time and the solvent diffusion coefficient in equilibrium conditions (indeed, solvent diffusion coefficient, according to eqs 2−4, is given by $D_r + D_0$ and, at equilibrium, $D_r = D_{eq} - D_0$ according to eq 5), respectively, and f and g are two model parameters. For each particle class "j" (particles having the same radius R_p) into which the continuous particle size distribution (see eq 1) can be subdivided, solvent mass balance reads

$$\frac{\partial C_{pj}}{\partial t} = \frac{1}{R_j^2} \frac{\partial}{\partial R_j}(-R_j^2 J_j) \quad (7)$$

Assuming that no volume variations occur upon polymer−solvent mixing (ideal behavior), particle volume increases and solvent concentration profile inside particles is evaluated on the basis of a microscopic (eq 7) and a macroscopic mass balance made up on each spherical shell (control volume[22]) into which the generic particle can be subdivided in (for each particle class "j" we have N_v control volumes). The macroscopic mass balance simply states that, at each time, the volume of the generic spherical shell is given by the sum of the polymer volume (constant with time) and the volume of the solvent contained in the spherical shell (local solvent amount). Obviously, local solvent volume depends on local solvent concentration that is time dependent. The spherical shell radius R_j depends on local solvent concentration according to

$$R_j = \sqrt[3]{R_{1j}^3 + [R_{2j}^3(0) - R_{1j}^3(0)]\frac{\rho_s}{\rho_s - C_{pj}}} \quad (8)$$

where ρ_s and C_{pj} are, respectively, solvent density and local concentration while R_{1j} and R_{2j} represent the radii of the inner and outer spherical shells sandwiching the spherical shell characterized by radius R_j. In addition, $R_{1j}(0)$ and $R_{2j}(0)$ indicate, respectively, the values of R_{1j} and R_{2j} when solvent concentration is zero (shrunken, dry condition).

Equations 7 are numerically solved[22] assuming that, initially, particles are solvent free, that solvent flux, for symmetry reasons, is zero in the particle center and solvent concentration at the particle surface is ruled by

(20) Tenchov, B. G.; Yanev, T. K. Weibull distribution of particle sizes obtained by uniform random fragmentation. *J. Colloid Interface Sci.* **1986**, *111*, 2–10.

(21) Camera-Roda, G.; Sarti, G. C. Mass transport with relaxation in polymers. *AIChE J.* **1990**, *36*, 851–860.

(22) Patankar, S. V. *Numerical Heat Transfer and Fluid Flow*; Hemisphere Publishing: New York, 1986.

$$\tau(C_{pj})\frac{dC_{pj}(t)}{dt}_{R=R_{pj}} = C_{peq} - C_{pj}(t) \qquad j = 1, 2, ..., N_c \tag{9}$$

where N_c is the number of classes into which the continuous particle size distribution (eq 1) has been subdivided and R_{pj} is the time dependent radius of particles belonging to class "j". Equation 9 states that at the particle surface ($R = R_{pj}(t)$), solvent concentration does not immediately reach the equilibrium value (C_{peq}) but its increase depends on the local relaxation time τ defined by eq 6.

The drug release process can be solved by writing a proper mass balance for each of the N_c classes into which the particle size distribution can be subdivided:

$$\frac{\partial C_j}{\partial t} = \frac{1}{R_j^2}\frac{\partial}{\partial R_j}\left(D\frac{\partial C_j}{\partial R_j}R_j^2\right) - \left(\frac{\partial C_{dj}^{am}}{\partial t} + \frac{\partial C_{dj}^{nc}}{\partial t} + \frac{\partial C_{dj}^{mc}}{\partial t}\right) \qquad j = 1, 2, ..., N_c \tag{10}$$

$$\frac{\partial C_{dj}^{am}}{\partial t} = \begin{cases} -K(C_s^{am} - C_j) & \text{if } C_{dj}^{am} > 0 \\ 0 & \text{if } C_{dj}^{am} = 0 \end{cases} \qquad j = 1, 2, ..., N_c \tag{11}$$

$$C_s^{am} = (C_{s0}^{am} - C_s^{mc})e^{-K_r t} + C_s^{mc} \tag{11'}$$

$$\frac{\partial C_{dj}^{nc}}{\partial t} = \begin{cases} -K(C_s^{nc} - C_j) & \text{if } C_{dj}^{nc} > 0 \\ 0 & \text{if } C_{dj}^{nc} = 0 \end{cases} \qquad j = 1, 2, ..., N_c \tag{12}$$

$$\frac{\partial C_{dj}^{mc}}{\partial t} = \begin{cases} -K(C_s^{mc} - C_j) & \text{if } C_{dj}^{mc} > 0 \\ 0 & \text{if } C_{dj}^{mc} = 0 \end{cases} \qquad j = 1, 2, ..., N_c \tag{13}$$

$$\frac{dM_c}{dt} = V_r K_{rb}(C_r - C_{sc}^{mc}) \tag{14}$$

where C_j is the concentration of the dissolved drug evaluated at radius R_j inside the particles of the jth class, C_{dj}^{am}, C_{dj}^{nc} and C_{dj}^{mc} are, respectively, the concentrations of the nondissolved drug in the amorphous, nanocrystalline and macrocrystalline states evaluated at radius R_j inside the particles of the jth class, D is the drug diffusion coefficient (depending on $C_{pj}(R_j)$), K rules the drug dissolution process inside each particle and it is independent of drug status (amorphous, nano- and macrocrystals),[23] C_s^{nc} and C_s^{mc} are, respectively, the drug nano- and macrocrystal solubility, V_r is the volume of the release environment and C_r is the drug concentration in the release environment. Equation 11′ expresses, according to the theory of Nogami,[23] the reduction of amorphous drug solubility at the solid−liquid interface. Indeed, upon dissolution, the amorphous phase recrystallizes on the solid surface in form of macrocrystals and the original amorphous surface is replaced by the macrocrystalline one. Consequently, amorphous drug solubility at the solid−solvent interface (C_s^{am}) reduces from the initial value C_{s0}^{am} to the final one C_s^{mc} according to the exponential law represented by eq 11′. While K_r rules drug recrystallization inside the particles, K_{rb} rules drug recrystallization in the release environment and M_c is the drug amount recrystallized in the release environment. It can be noted that in the drug mass balance referred to the jth particle class (eq 10), four contributions appear in the right-hand side term. While the first one is related to the diffusion process, the following three represent, respectively, the dissolution process of amorphous, nanocrystalline and macrocrystalline drug. The dissolution process of the nondissolved drug in its three possible conditions (amorphous, nanocrystalline and macrocrystalline) is represented by eqs 11−13, whose right-hand side term is set to zero when C_{dj}^{am}, C_{dj}^{nc} and C_{dj}^{mc} disappear (solid drug has completely solubilized).

As the drug diffusion coefficient in the polymeric network mainly depends on the local solvent concentration, the D dependence on C_p suggested by Peppas and Reinhart[24,25] is considered:

$$\frac{D}{D_{ds}} = e^{-B\varphi/(1-\varphi)}, \qquad \varphi = 1 - \frac{C_p}{\rho_s} \tag{15}$$

where D_{ds} is the drug diffusion coefficient in the pure solvent, B is a model parameter while φ is the local polymer volume fraction and ρ_s is the solvent density. Equation 10 is numerically solved[22] assuming that the initial drug concentration in the release environment is zero, that, initially, no dissolved drug exists inside the particles (only solid or amorphous drug can be found in the polymeric network) and that the solid and/or amorphous drug concentration is uniform inside the particles (the model could easily account for more complex drug distributions). Finally, for symmetrical reasons, drug flux in the particle's center is set to zero and the usual drug partitioning condition at the particle/solvent interface is considered (K_p is the drug partition coefficient).

In order to complete the model, the equations related to drug absorption, distribution and elimination must be considered. For this purpose, it is convenient to refer to Figure 1, which reports the physical situation that the model mimics.

Drug concentration in the blood (C_b) increases due to the drug flux coming from the GI tract fluid and crossing the GI mucosa ($AP(C_r - C_b)$). At the same time, C_b decreases because of the elimination/metabolism process ($-K_{el}^* C_b$) and it is affected by the distribution within the surrounding tissues/organs ($-K_{12}^* C_b + K_{21}^* C_T$; C_T = drug concentration inside tissues/organs). Thus the differential equation accounting for C_b variation is

(23) Nogami, H.; Nagai, T.; Youtsuyanagi, T. Dissolution phenomena of organic medicinals involving simultaneous phase changes. *Chem. Pharm. Bull.* **1969**, *17*, 499–509.

(24) Peppas, N. A.; Reinhart, C. T. Solute Diffusion in Swollen Membranes. I. A New Theory. *J. Membr. Sci.* **1983**, *15*, 275–287.

(25) Reinhart, C. T.; Peppas, N. A. Solute Diffusion in Swollen Membranes. II. Influence of Crosslinking on Diffusive Properties. *J. Membr. Sci.* **1984**, *18*, 227–239.

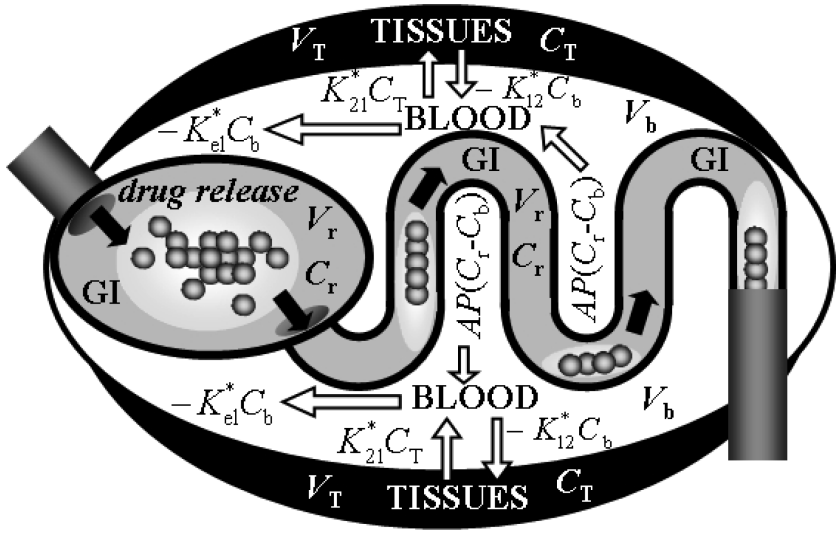

Figure 1. Schematic representation of drug release (from drug loaded polymeric particles), absorption, elimination/metabolism and exchange with tissues.

$$V_b\frac{dC_b}{dt} = AP(C_r - C_b) - K^*_{el}C_b - K^*_{12}C_b + K^*_{21}C_T \tag{16}$$

where t is time and V_b, A and P are, respectively, the blood compartment volume, the GI tract geometrical surface (without considering the presence of villi and microvilli that would considerably increase the surface) and the average apparent permeability of the GI tract. The adjective "apparent" is due to the fact that P does not refer to the real absorption surface of the GI but to the geometrical one. Nevertheless, as the product AP is equal to the product of real permeability and surface area, in principle, there is no need for the exact knowledge of real A and P. Analogously, the variation of drug concentration inside tissues/organs C_T is given by

$$V_T\frac{dC_T}{dt} = K^*_{12}C_b - K^*_{21}C_T \tag{16a}$$

where V_T is the tissue/organ volume while K^*_{12} and K^*_{21} are, respectively, the direct and reverse exchange constants between the blood and the tissue/organ compartments. The above-mentioned equations can be conveniently rewritten as

$$\frac{dC_b}{dt} = K_a(C_r - C_b) - K_{el}C_b - K_{12}C_b + K_{12}C_T \tag{17}$$

$$\frac{dC_T}{dt} = K_{12}fC_b - K_{21}fC_T \tag{18}$$

where the absorption constant is defined by $K_a = AP/V_b$, the elimination constant is defined by $K_{el} = K^*_{el}/V_b$, the exchange constants are defined by $K_{12} = K^*_{12}/V_b$ and $K_{21} = K^*_{21}/V_b$ and $f = V_b/V_T$.

In order to close the balance between the unknowns (drug concentration profile inside each particle class, C_r, C_b, and C_T) and the equations, we need one more equation. This equation is an overall mass balance ensuring that the sum of the drug mass present in the GI fluid (V_rC_r), in the delivery system ($\sum_{j=1}^{N_c}N_{pj}\int_0^{R_{pj}}$ $[C_j(R_j) + C^{am}_{dj}(R_j) + C^{nc}_{dj}(R_j) + C^{mc}_{dj}(R_j)]4\pi R_j^2\,dR_j$), in the blood ($V_bC_b$), in tissues/organs ($V_TC_T$) plus the amount of drug recryst alliz ed in the release environment (M_c) and that eliminated/metabolized in the blood (M_e) is always equal to the initial drug mass administered, i.e. drug dose (M_0):

$$M_0 = V_rC_r + \sum_{j=1}^{N_c}N_{pj}\int_0^{R_{pj}}[C_j(R_j) + C^{am}_{dj}(R_j) + C^{nc}_{dj}(R_j) + C^{mc}_{dj}(R_j)]4\pi R_j^2\,dR_j + V_bC_b + V_TC_T + M_c + M_e \tag{19}$$

$$M_e = \int_0^t K_{el}V_bC_b\,dt \tag{19'}$$

where V_r is the release environment volume and N_{pj} indicates the number of particles belonging to the "j" class. While eqs 7 and 10 are solved according to the fully implicit control volume method[22] assuming $N_v = 10$, $N_c = 20$ and a time step of 2.5 s, ordinary differential equations (eqs 17, 18) are solved by considering an implicit finite difference approach.

3.2. Evaluation of Model Parameters. As the presented model needs many parameters, the majority of them have to be determined in advance in order to minimize the number of fitting parameters. Accordingly, the parameters ruling solvent uptake are set according to previous findings:[4] $C_{peq} = 0.31$ g/cm^3, $D_{eq} = 10^{-7}$ cm^2/s, $D_0 = 10^{-10}$ cm^2/s, $g = 51.75$, $\tau_{eq} = 0.35$ and $f = 12$. Particle size distribution can be described by eq 1 assuming $\eta = 60 \times 10^{-4}$ cm, $\delta = 1$ and 10^{-4} cm $\le R_p \le 140 \times 10^{-4}$ cm.[11] Vinpocetine physical properties were determined elsewhere[11] and are reported in Table 1. While, for the sake of simplicity, the vinpocetine partition coefficient (K_p) is set to 1, its diffusion coefficient

Table 1. Vinpocetine Physicochemical Characteristics[a]

M_w	pK_b	C_s^{mc}(μg/cm^3) (37 °C, buffer, pH = 7.4)		
350	7.3		1.6	
ρ_s (kg/m^3)	ρ_l (kg/m^3)	T_m (°C)	ΔH_m (J/kg)	ΔC_{pls}(J/kg K)
1268	1217	149.6	94600	374
γ_{sl} (mJ/m^2)	γ_{lv} (mJ/m^2)	γ_{sv} (mJ/m^2)	θ_{H2O} (deg)	θ_{CH2I2} (deg)
8.9	29.5	38.4	81	33

[a] M_w is the drug molecular weight, pK_b indicates the pH value for vinpocetine dissociation, C_s^{mc} is the solubility, ρ_s and ρ_l are, respectively, the solid and liquid density, T_m and ΔH_m are, respectively, the melting temperature and enthalpy, ΔC_{pls} is the difference between the specific heat at constant pressure in the liquid and solid state, γ_{sl} is the solid−liquid vinpocetine surface tension, γ_{lv} is the liquid−vapor vinpocetine surface tension, γ_{sv} is the solid−vapor vinpocetine surface tension, θ_{H2O} and θ_{CH2I2} are, respectively, the water and diiodemethane contact angles on solid vinpocetine.[11]

in water at 37 °C is evaluated according to the well-known Stokes−Einstein equation ($D_{ds} = 4.7 \times 10^{-6}$ cm^2/s). In addition, the parameter B of eq 15 is set to 1.[26]

Finally, the determination of vinpocetine nanocrystals solubility (C_s^{nc}) is needed. Unfortunately, this information cannot be experimentally retrieved because of many factors, among which Ostwald ripening[4] is one of the most important. This phenomenon consists of larger crystal growth at the expense of smaller and the asymptotic reduction of solution solubility. Indeed, the dissolution of small crystals, characterized by higher solubility, renders the liquid phase oversaturated with respect to big crystals, characterized by lower solubility. Thus, part of the solute leaves the solution and provokes bigger crystal growth. This is the reason why the estimation of C_s^{am} can be performed only on a theoretical basis. The starting point is the thermodynamic equation representing the equilibrium between a liquid and a nanocrystalline solid phase, in the hypothesis that the liquid phase does not spread in the solid one:

$$X_d = \frac{f_d^s}{f_d^l}\frac{1}{\gamma_d} \qquad C_s^{nc} = \frac{X_d}{1 - X_d}\frac{M_w}{M_{ws}}\rho_s \tag{20}$$

where γ_d and X_d are, respectively, the drug activity coefficient and solubility (molar fraction) in the liquid phase, f_d^l is the drug fugacity in the reference state, f_d^s is the drug fugacity in the nanocrystalline solid state and M_{sw} is the solvent molecular weight. Assuming f_d^l as the fugacity of pure drug in the state of undercooled liquid at the system temperature (T) and pressure, eq 20 becomes[4]

$$A_1 = \Delta C_{pls}(T - T_{mr}) + \Delta H_{mr} \tag{21a}$$

$$A_2 = T(\Delta C_{pls}\ln(T/T_{mr}) + \Delta H_{mr}/T_{mr}) \tag{21b}$$

$$X_d = \frac{1}{\gamma_d}\exp\left(-\frac{A_1 - A_2}{RT}\right) \tag{21}$$

where T_{mr} and ΔH_{mr} are, respectively, nanocrystals melting temperature and enthalpy. The determination of T_{mr} and ΔH_{mr} relies on the relations existing among T_{mr}, ΔH_{mr} and the nanocrystals radius R^{nc}:[4]

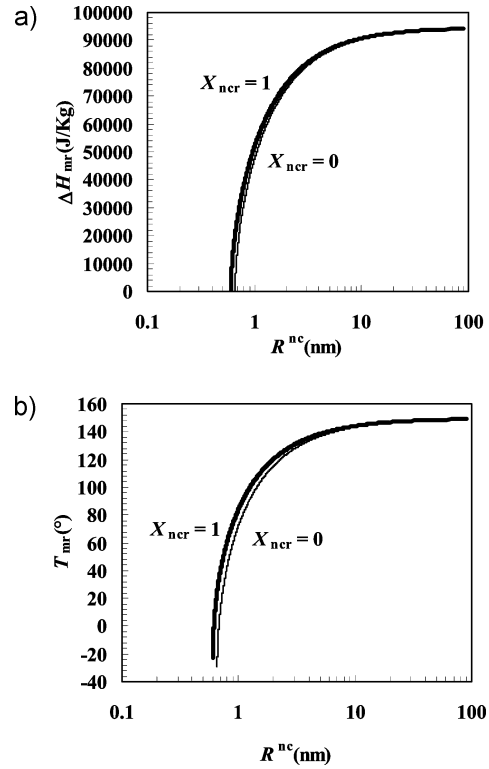

Figure 2. (a) Vinpocetine melting enthalpy (ΔH_{mr}) reduction with nanocrystals radius R^{nc} for different values of the nanocrystals mass fraction (X_{ncr}). (b) Vinpocetine melting temperature (T_{mr}) reduction with nanocrystal radius R^{nc} for different values of the nanocrystal mass fraction (X_{ncr}).

$$\int_{T_m}^{T_{mr}}\frac{\Delta H_{mr}}{T}\,dT = -\frac{2}{R^{nc}}\left\{X_{ncr}\left(\frac{\gamma_{sl}}{\rho_s} + \gamma_{lv}\left(\frac{1}{\rho_s} - \frac{1}{\rho_l}\right)\right) + (1 - X_{ncr})\frac{\gamma_{sl}}{\rho_s}\right\} \tag{22}$$

$$\Delta H_{mr} = \Delta H_m - \frac{3}{R^{nc}}\left(\frac{\gamma_{sv}}{\rho_s} - \frac{\gamma_{lv}}{\rho_l}\right) - \Delta C_{pls}(T_m - T_{mr}) \tag{23}$$

where X_{ncr} indicates the mass fraction of nanocrystals constituting the solid phase (the remaining part of the solid phase is represented by amorphous drug that cannot melt). While eq 22 is a modification of the Brun theory,[27] the second one (eq 23) is the equation of Zhang.[28] The simultaneous, iterative, numerical solution of eqs 22 and 23 allows the determination of the T_{mr} and ΔH_{mr} dependence on R^{nc} once X_{ncr} is fixed (see Figure 2a,b). On this basis and

(26) Grassi, M.; Lapasin, R.; Coviello, T.; Matricardi, P.; Di Meo, C.; Alhaique, F. Scleroglucan/borax/drug hydrogels: Structure characterisation by means of rheological and diffusion experiments. *Carbohydr. Polym.* **2009**, *78*, 377–383.

(27) Brun, M.; Lallemand, A.; Quinson, J. F.; Eyraud, C. Changement d'etat liquide−solide dans les milieux poreux. *J. Chim. Phys.* **1973**, *70*, 979–989.

(28) Zhang, M.; Efremov, M. Y.; Schiettekatte, F.; Olson, M. Y.; Kwan, A. T.; Lai, S. L.; Wisleder, T.; Greene, J. E.; Allen, L. H. Size-dependent melting point depression of nanostructures: nanocalorimetric measurements. *Phys. Rev. B* **2000**, *62*, 10548–10557.

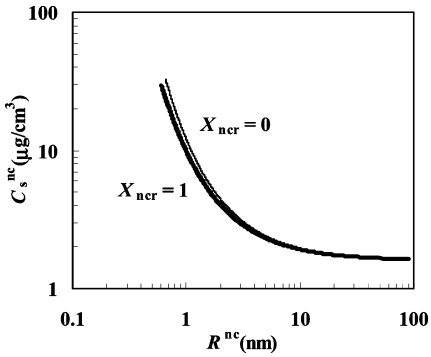

Figure 3. Dependence of vinpocetine solubility (C_s^{nc}) on the dimension of nanocrystal curvature radius (R^{nc}) for different values of the nanocrystal mass fraction (X_{ncr}).

knowing that $X_d = 5.27 \times 10^{-8}$ mol/L (= 1.6 μg/mL), it is possible estimating $\gamma_d = 911460$. Assuming that γ_d does not modify with R^{nc}, it is possible to estimate the dependence of vinpocetine nanocrystals solubility on R^{nc} according to eq 19 (see Figure 3). Figures 2 and 3 make clear that the variation of nanocrystal mass fraction (X_{ncr}) does not sensibly affect the trend of vinpocetine melting enthalpy (ΔH_{mr}), melting temperature (T_{mr}) and solubility (C_s^{nc}) versus nanocrystal radius (R^{nc}).

4. Results

Due to model complexity, the study of the *in vivo* behavior of our coground system needs to fit in advance the model to *in vitro* data in order to determine three very important model parameters, namely, the amorphous vinpocetine solubility (C_{s0}^{am}), dissolution (K) and recrystallization (K_r, K_{rb}) constants. Essential prerequisite for *in vitro* data fitting is the determination of drug condition inside the coground system, i.e. the fraction of vinpocetine present in form of macrocrystals, nanocrystals and amorphous drug. On the basis of the thermal behavior of the coground system (obtained by differential scanning calorimeter analysis[11]) and the data shown in Table 1, eqs 22 and 23 can be iteratively solved to determine the mass fraction of nanocrystals (X_{ncr}). In particular, we find that vinpocetine macrocrystals are absent (no melting peak appeared at 149.6 °C) while the mass fraction (X_{ncr}) of nanocrystalline vinpocetine is 0.17, the remainder being amorphous vinpocetine (0.83). As the average nanocrystalline radius R^{nc} is equal to 5 nm, it can be concluded that vinpocetine nanocrystal solubility C_s^{nc} is, approximately, 2.4 μg/cm^3 (see Figure 3). Knowing the information on the vinpocetine state in the coground system, drug concentration in the particles ($C_{dj}^{am} = 211060$ μg/cm^3; $C_{dj}^{nc} = 31537$ μg/cm^3; $C_{dj}^{mc} = 0$ μg/cm^3; $j = 1, ..., N_c$) and assuming the values of all other model parameters as previously set (see sections 2.2 and 3.2), the model can be fitted to *in vitro* data referring to 5 mg dose (open circles in Figure 4). Obviously, at this stage, model fitting is performed setting all the pharmacokinetic constants equal to zero as no ADME processes take place in the *in vitro* test. Figure 4 reports the comparison between model best fitting (solid thick line) and the *in vitro* experimental results referring to 5 mg dose (open circles).

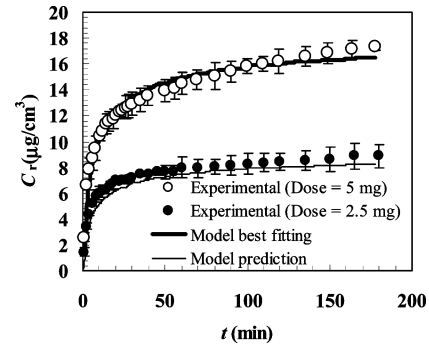

Figure 4. Vinpocetine concentration increases (C_r) in the release environment in *in vitro* test. Open circles indicate the experimental data referring to a drug dose of 5 mg while filled circles indicate the experimental data referring to a drug dose of 2.5 mg (vertical bars indicate standard error). Solid thick line indicates model best fitting while solid thin line represents model prediction determined on the basis of parameters determined by model fitting to 5 mg dose data.

It can be seen that the fitting is satisfactory as also proved by the statistical F-test ($F(1,10,95) < 945$). Fitting parameters read $K_r = K_{rb} = 0$, $KC_{s0}^{am} = 1000 \pm 100$ μg/cm^3. Unfortunately, the absence of macrocrystals and the relatively small fraction of nanocrystals make parameters K and C_{sa} highly correlated (see eqs 11−13). Accordingly, we can estimate only their product setting $K = 1$ s^{-1} and letting C_{s0}^{am} to change during the fitting procedure. However, the correctness of these findings is proved by the comparison between model prediction (solid thin line in Figure 4) and release data referring to 2.5 mg dose (filled circles in Figure 4). Model prediction is obtained by assuming all the parameters coming from model fitting to 5 mg dose data except for the amount of the coground system that is one-half. Relying on these findings, it is possible to fit the model on *in vivo* data assuming that the volume of the release environment V_r (GI fluids) is equal to 250 cm^3 [29] and knowing that the dose (M_0, see eq 19) is equal to 10 mg (this corresponds to 50 mg of the coground system). Figure 5a shows, for each one of the eight volunteers considered in this study, the time course of vinpocetine concentration in the blood (C_b) after oral administration of 50 mg of the coground system, corresponding to a dose of 10 mg of vinpocetine.

In order to check its reliability also in the *in vivo* case, the model is fitted on the experimental subset represented by the first five volunteers (open circles in Figure 5b, sampling at 0.5, 1, 2, 4, and 6 h) and then this fitting is compared with the other experimental subset represented by the remaining three volunteers (filled circles in Figure 5b, sampling at 0.25, 0.5, 1, 1.5, 2, 3, 4, and 6 h). In so doing, we can evaluate the general validity of model findings on other, uncorrelated subjects, and we can see the model reliability in predicting the vinpocetine blood concentration

(29) Macheras, P.; Iliadis, A. *Modeling in biopharmaceutics, pharmacokinetics and pharmacodynamics—homogeneous and heterogeneous approaches*; Springer: New York, 2006; pp 113−117.

Table 2. Age, Sex and Weight of the 8 Healthy, Male Volunteers Involved in This Study

N	age (years)	wt (kg)
1	25	72
2	50	75
3	31	78
4	26	68
5	31	85
6	45	77
7	39	81
8	28	77
average ± SD	34 ± 9	77 ± 5

corresponding to sampling times (0.25, 1.5, and 3 h) different from those used (0.5, 1, 2, 4, and 6 h) for model fitting.

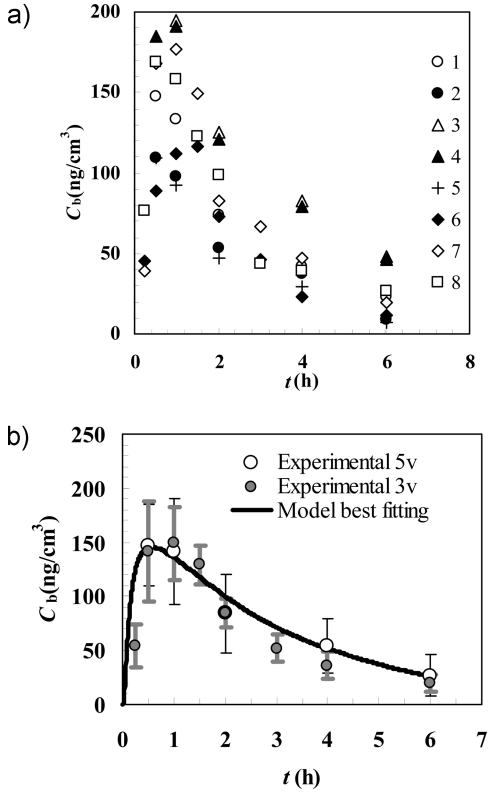

Figure 5. (a) Time course of vinpocetine concentration in the blood (C_b) after oral administration of 50 mg of the coground system, corresponding to a dose of 10 mg of vinpocetine (17% nanocrystalline and 83% amorphous). Each symbol represents one volunteer whose characteristics are listed in Table 2. (b) Time course of vinpocetine concentration in the blood (C_b) after oral administration of 50 mg of the coground system, corresponding to a dose of 10 mg of vinpocetine (17% nanocrystalline and 83% amorphous). Open circles indicate the experimental data on which the model was fitted to, while gray circles serve to check the reliability of the model prediction. Model best fitting is represented by the continuous line, and vertical bars indicate datum standard error.

A preliminary fitting procedure led on the first experimental subset (open circles in Figure 5b), assuming V_b, V_T, K_a, K_{el}, K_{12} and K_{21} as fitting parameters, reveals that K_{12} and K_{21} are unnecessary as they turn out to be statistically not different from zero. Accordingly, data fitting is repeated assuming V_b, K_a and K_{el} as fitting parameters. In order to speed up the fitting procedure (we are dealing with a mathematical model requiring a heavy numerical solution), model fitting is led fixing V_b and allowing K_a and K_{el} to vary in order to minimize χ^2.

This procedure is repeated for different values of V_b starting from an initial guess determined by fitting the *in vivo* data referring to the first blood concentration C_b measured at 1, 2, 4, and 6 h (first five volunteers; see Figure 5b) by means of a simple C_b exponential decay with time:

$$C_b = \frac{M_0}{V_b} \exp(-K_{el}t) \tag{24}$$

Basically, this equation assumes that drug elimination is the leading process after 1 h. Accordingly, V_b first guess is V_b^{fg} = (55000 ± 6000) cm^3 (we also find that K_{el} = (0.32 ± 0.04) h^{-1}). Whereas χ^2 increases for $V_b > V_b^{fg}$, it decreases for smaller values up to a critical V_b value, after which further V_b decrease leads to χ^2 increase. Assuming V_b critical value as the true one, model fitting results in V_b = 36200 cm^3, K_a = (0.11 ± 0.6) h^{-1} and K_{el} = (0.5 ± 0.03) h^{-1}. As Figure 5b clearly shows, the fitting (solid line) is accurate, as also indicated by the *F*-test result ($F(1,3,0.95) < 165$). In addition, the comparison between model best fitting (solid line) and the second subset of experimental data (gray circles) indicates a general agreement between them also in the case of sampling performed at 0.25, 1.5, and 3 h.

5. Discussion

An inspection of Figure 3 reveals that, regardless of nanocrystal mass fraction X_{ncr}, an interesting increase of vinpocetine solubility takes place only for nanocrystal radius smaller than 2 nm. For smaller radii, solubility increases up to around 35 μg/cm^3 (approximately 22 times that of the original macrocrystalline vinpocetine), this corresponding to the half side of the smallest vinpocetine crystal, i.e. the crystalline unit cell (~0.6 nm).[11] Although we could not separately determine amorphous vinpocetine solubility (C_{s0}^{am}) and dissolution constant (K), Figure 3 would suggest that the assumption $C_{s0}^{am} \approx 1000$ μg/cm^3 is not so unreasonable. In addition, for the *in vivo* fitting, we do not need an exact knowledge of both K and C_{s0}^{am} as, in our case (absence of macrocrystals and predominance of amorphous fraction on the nanocrystalline one), drug dissolution is essentially ruled by the product KC_{s0}^{am} (see eqs 11−13). In the light of these considerations, we can conclude that a real improvement of vinpocetine solubility occurs essentially when it is reduced to its amorphous state. The results coming from the model fitting on the experimental *in vitro* data make clear that the vinpocetine recrystallization process is very slow as a vanishing K_r value turns out for the description of three hours

lasting experiments (Figure 4). Although recrystallization will surely occur at longer time points, its importance on *in vivo* behavior is very limited as after three hours the predominant part of the absorption process has been completed (see Figure 5a,b).

The value of V_b, bigger than the theoretical blood volume ($\sim$3250 cm^3 for a human being weighing 75 kg[30]), can be explained by vinpocetine binding to plasma proteins.[18] The vinpocetine elimination constant ($K_{el} = 0.5$ h^{-1}) results as comparable to that of acetaminophen (0.28 h^{-1}), gentamicin (0.35 h^{-1}) and lidocaine (0.43 h^{-1}) while it is neatly bigger than that of diazepam (0.021 h^{-1}), digoxin (0.017 h^{-1}) and theophylline (0.063 h^{-1}).[31] Finally, the evaluation of the absorption constant ($K_a = AP/V_b$) allows the estimation of the vinpocetine apparent permeability P as blood volume (V_b) has been determined and the GI tract geometrical surface A is around 13116 cm^2.[4] Accordingly we have $P \approx 8 \times 10^{-5}$ cm/s, this putting vinpocetine in the class II drugs (poor solubility and good permeability) according to the Amidon biopharmaceutics classification.[29,32]

(30) Berezhkovskiy, L. M. Determination of Mean Residence Time of Drug in Plasma and the Influence of the Initial Drug Elimination and Distribution on the Calculation of Pharmacokinetic Parameters. *J. Pharm. Sci.* **2008**, *98*, 748–762.

(31) Ritschel, W. A. *Handbook of Basic Pharmacokinetics*; Drug Intelligence Publications: Hamilton, IL, 1980; 2nd ed. pp 413−426.

(32) Amidon, G.; Lennernas, H.; Shah, V.; Crison, J. A theoretical basis for a biopharmaceutic drug classification: the correlation of in vitro drug product dissolution and in vivo bioavailability. *Pharm. Res.* **1995**, *12*, 413–420.

6. Conclusion

This work proves that it is possible to build up a mathematical model able to describe the *in vivo* fate of a drug orally administered. In particular, the proposed model can account for the simultaneous processes of *in vivo* drug release and ADME processes following the oral administration of a drug dispersed, in the form of nanocrystals and amorphous state, inside polymeric particles of different dimensions. For this purpose, the model needs the knowledge of information on the polymer and drug physicochemical properties. In addition, some fitting parameters have to be determined by model fitting to *in vitro* release data. Once all the parameters are known, it is possible to use the model to predict or, at least, to give a reasonable idea of the effect of the different parameters on the time course of the drug concentration in the blood. Accordingly, this model should be an important tool helping to drive and to focus experimental tests to a fixed target, saving money and time. Future development of this model will focus on the variation of both drug solubility and permeability through the GI tract.

Acknowledgment. This work has been supported by the Italian Ministry of Education (PRIN 2008 (2008HCAJ9T)) and by the "Fondazione Benefica Kathleen Foreman Casali" of Trieste.

MP1001334